Technical Sciences
Academy of Romania
www.jesi.astr.ro

Journal of Engineering Sciences and Innovation
Volume 4, Issue 3 / 2019, pp. 285-300
http://doi.org/10.56958/jesi.2019.4.3.285

B. Chemical Engineering, Materials Science and Engineering

Received 8 July 2019 Accepted 3 September 2019
Received in revised from 26 August 2019

Thermodynamics of in situ formation of TiB_2 particulates in complex aluminium alloys for aeronautics

PETRU MOLDOVAN, MIHAI BUŢU*

Polytechnica University of Bucharest, Splaiul Independentei nr. 313, Bucharest, Romania

Abstract. Aluminum complex alloy AlCuMgZn, reinforced by in-situ TiB_2 particles are fabricated via liquid metallurgy route based on the exothermic reactions between matrix alloy and inorganic salt mixture (K_2TiF_6 and KBF_4), at 750ºC, at various time (60, 90 and 120 minutes). The XRD patterns revealed the formation of TiB_2. At working temperature by thermodynamic point of view (negative ΔG), some secondary reaction also was possible, and AlB_{12}, MgB_2 and MgB_{12} can to form. The main alloying elements of AlCuMgZn alloy do not influence final reaction products. Increasing the reaction time from 60 to 120 minutes leads to agglomeration of TiB_2 particles. Form and dimensions of TiB_2 particles obtained after separation from aluminium matrix were determined by Transmission Electron Microscopy (TEM) and through Dynamic Light Scattering (Zetasizer Nano ZS Malvern).

Keywords: in-situ AlCuMgZn - TiB_2 composites, thermodynamics, TiB_2 particles, TEM, Dynamic Light Scattering (DLS).

1. Introduction

Aluminium matrix composites (AMCs) are very attractive materials in recent years. Discontinuously reinforced AMCs results in improved physical and mechanical properties that cannot be achieved using conventional engineering alloys. The progress in production techniques enabled researches to synthesize AMCs composites reinforced with various oxides, carbides and nitrides (Al_2O_3, TiC, TiB_2, ZrB_2 and AlN) particulates [1, 2].

In-situ fabrication of AMCs is a process, in which reinforcing phase is formed in the aluminium matrix gives better physical and mechanical properties than ex-situ AMCs due to good matrix / particle interface and finer reinforcement particles size

* Correspondence address: mihaibutu@yahoo.com

[2-7]. In the last years have been realized many researches based on the exothermic reactions between the aluminium alloys (as matrix) and salt mixtures (KBF_4 + K_2TiF_6) [3, 5-15].

However, information related to the thermodynamics and also the characterization of $TiAl_3$ and TiB_2 particulates which is formed in this type of composites is very limited [4, 11, 12].

The objective of this paper is to present our results of the thermodynamics of in-situ TiB_2 particulates formed in Al-Cu-Mg-Zn / metallic boride composites.

Alloys from the quaternary system Al-Cu-Mg-Zn displays outstanding properties both as cast and after machining and specific heat. However, this system is not sufficiently studied, although it is used in high-tech industries, especially because of the large main alloying elements [16].

However, the fundamental understanding of the (Al) corner of this diagram, in particular, the liquidus projections and solidification surface are absent. For this reason, figure 1 represents the results obtained by the authors [16] based on many years of joint work upon this subject. Table 1 provides the corresponding non-variant phase reactions. One should mention that the latter take place at concentrations, which are quite different from those corresponding to known industrial alloys. For this reason, the most valuable information is contained in the isothermal cross-sections provided in figure 1 [16].

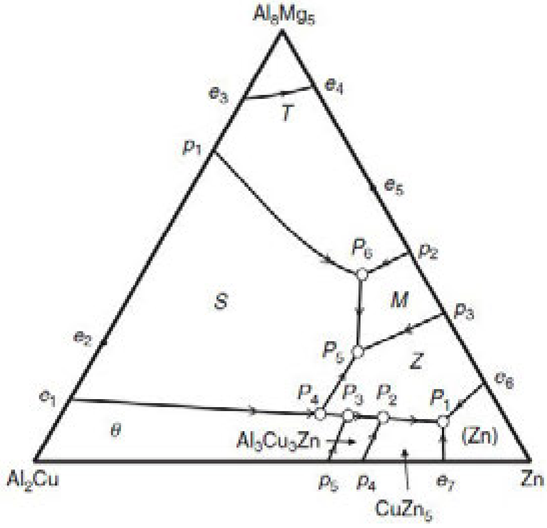

Fig. 1. Phase diagram Al-Cu-Mg-Zn: single-phase domains [16].

The $CuMg_4Al_6$ and $Mg_3Zn_3Al_2$ phases in ternary systems exist in a broad range of concentrations. In the quaternary system the phase domain occupied by the quaternary solid solution (the T-phase - cubic structure) is also quite broad (figure 1). The quaternary solid solution between compounds CuMgAl and $MgZn_2$ (the so-called M-phase) is characterized by hexagonal structure.

Table 1. Non-variant reactions in quaternary alloys of the Al-Cu-Mg-Zn system [16]

Point in figure 1	Phase reaction	Composition of liquid			T°C
		Zn(%)	Mg(%)	Cu(%)	
P_1	L + Cu Zn_5 ⇒ (Al) + (Zn) + Z	91.1	2.2	3.4	350
P_2	L + Cu_3ZnAl_3 ⇒ (Al) + $CuZn_5$ + Z	82.6	5.4	10.1	363
P_3	L + Al_2Cu ⇒ (Al) + Cu_3ZnAl_3 + Z	77.2	3.0	9.8	377
P_4	L + Al_2CuMg + Al_2Cu ⇒ (Al) + Z	6.5	6.5	38.9	482
P_5	L + Al_2CuMg ⇒ (Al) + Z + M	-	-	-	< 467
P_6	L + T ⇒ (Al) + Al_2CuMg + M	-	-	-	< 467

The solid solution formed by $Cu_6Mg_2Al_5$ and Mg_2Zn_{11} compounds (the Z-phase - cubic structure). The $CuAl_2$ phase practically does not dissolve magnesium and dissolves not more than 2% Zn. The $CuMgAl_2$ phase also has very limited solubility range and can dissolve less than 1% Zn. In alloys containing 4 ÷ 8% Zn and 0.5 ÷ 1.0% Cu, the lattice parameter increases with Mg content in solid solution [16].

2. Experimental procedure

In-situ composites with TiB_2 particles were fabricated in an electric furnace using a graphite clay crucible by direct reaction between complex aluminium melt and mixed salts KBF_4, K_2TiF_6 and Na_3AlF_6, at 750 ÷ 950°C. A preweighted mixture of inorganic salts was added into the molten metal using the stirring method.

Cryolite (Na_3AlF_6) was added for the metal bath protection and dissolution of the formed oxides. The characteristic of the salts and metals used are following:

- Potassium hexafluorotitanate (K_2TiF_6): molecular weight: 240.09 g/mol; appearance: white crystalline flakes; melting point: 780°C; composition: 99% min.; Cl ≤ 0.05%; SO_4 ≤ 0.01%; H_2O ≤ 0.05%; Pb ≤ 0.01%; SiO_2 ≤ 0.2%; Fe ≤ 0.02%; grit: 60 mesh - 5% max.; 200 mesh - 45 % min.; 300 mesh - 20% max.;
- Potassium tetrafluoroborate (KBF_4): molecular weight: 125.91 g/mol; density (20°C): 2.5 g/cm^3; volumetric weight: 800 ÷ 1400 g/l; molar volum: 49.4 cm^3; melting point: 530°C; solubility in water (20°C): 4.4 g/l; composition: > 98%; Fe ≤ 0.01%; SO_4 ≤ 0.02%; SiO_2 ≤ 0.4%; Cl ≤ 0.1%; Pb ≤ 0.0005%; Na ≤ 0.1%; Mg ≤ 0.05%; H_2O (110°C) ≤ 0.05%;
- Cryolite (Na_3AlF_6): molecular weight: 209.94 g/mol; appearance: white powder; density (20°C): 2.95 g/cm^3; volumetric weight: 600 ÷ 1000 g/l; melting point: 1027°C; solubility in water (20°C): 0.42 g/l; composition: Na 30 ÷ 32%; Al 12 ÷ 13.5%; F ≥ 53.0%; Fe ≤ 0.03%; SO_4 ≤ 0.5%; SiO_2 ≤ 0.25%; P_2O_5 ≤ 0.03%; Cl ≤ 0.1%; Pb ≤ 0.0005%.
- AA 7xxx series aluminium alloys

Table 2. Chemical composition of 7xxx alloys, wt% [12]

Alloy	Si	Fe	Cu	Mn	Mg	Cr	Zn	Ti	Zr	Al
EN AW 7050 AlZn6CuMgZr	0.12	0.15	2.0 ÷ 2.6	0.10	1.9÷ 2.6	0.04	5.7 ÷ 6.7	0.06	0.08 ÷ 0.15	rest
7050 - sample C	0.065	0.11	2.20	0.021	2.28	0.0025	5.95	0.035	0.09	rest

After the slag is removed, the composite was poured into cast iron mould in the form of bars of 10 mm diameter. The specimens from the cast composites were polished and etched with Keller reagent and examined by OM (optical microscopy) and X-ray diffractometer.

Samples of the composite materials was dissolved in concentrated HCl and powder of TiB_2 particle was examined using X-ray diffractometer.

3. Results and discussions

The studies presented in the literature refers specifically to less complex systems [2, 3, 5-10, 13-15], in terms of development and in-situ growth of particle reinforcement. For complex systems Al-Cu-Mg-Zn / K_2TiF_6 / KBF_4 [4, 11, 12] is interesting to see whether high concentrations of Cu (> 1.5%), Mg (> 2.2%) and Zn (> 5.4%) influence the final reaction products for reactions (1 ÷ 9).

According to calculation by T. Fan, G. Yang, and D. Zhang [10] results that free excess energy of TiB_2, and Al_3Ti formation may be influenced by various alloying elements in aluminium. Thus, the addition of Mg, Cu, Zn, Ni, Fe, V and La may intensify the formation of Al_3Ti and TiB_2.

To highlight the thermodynamics of boride particle formation in aluminium complex 7xxx alloys, three times to react for produce TiB_2 (60, 90 and 120 minutes) were studies. From thermodynamic studies results 14 reactions, the aluminothermic reduction of salts (K_2TiF_6 and KBF_4) occurs:

$$3K_2TiF_6 + 13Al = 3Al_3Ti + 6KF + 4AlF_3 \quad (1)$$

$$3K_2TiF_6 + 6KBF_4 + 10Al = 12KF + 10AlF_3 + 3TiB_2 \quad (2)$$

$$6KBF_4 + 9Al = 3AlB_2 + 6KF + 6AlF_3 \quad (3)$$

$$12KBF_4 + 13Al = AlB_{12} + 12KAlF_4 \quad (4)$$

$$12KBF_4 + 13Al = AlB_{12} + 12KF + 12AlF_3 \quad (5)$$

$$K_2TiF_6 + 2KBF_4 + 5Mg = 4KF + 5MgF_2 + TiB_2 \quad (6)$$

$$2Al + 2KBF_4 + Mg = MgB_2 + 2KF + 2AlF_3 \quad (7)$$

$$12Al+ 12KBF_4 + Mg = MgB_{12} + 12KAlF_4(g) \quad (8)$$

$$12Al+ 12KBF_4 + Mg = MgB_{12} + 12KF + 12AlF_3 \quad (9)$$

Thermodynamic data computed with HSC Chemistry program indicates, in the temperature range 750 ÷ 950°C, possibility of Al_3Ti, TiB_2, AlB_2, AlB_{12}, MgB_2 and MgB_{12} compounds formation, with negative ΔG^o_T (table 3 for reactions 1 ÷ 7 and table 4 for reactions 8 ÷ 14).

At the working temperature, in the condition of exothermic reaction heat evolution, the Al_3Ti, TiB_2, AlB_2, AlB_{12}, MgB_2 and MgB_{12} particles developed from reaction (1 ÷ 9), can react resulting in-situ Al_3Ti / TiB_2 reinforced compound of aluminium matrix:

$$AlB_2 + Al_3Ti = TiB_2 + 4Al \quad (10)$$

$$AlB_{12} + Al_3Ti + Al = TiB_2 + 5AlB_2 \quad (11)$$

$$MgB_{12} + Al = AlB_{12} + Mg \quad (12)$$

$$MgB_{12} + 5Mg = 6MgB_2 \quad (13)$$

$$AlB_{12} + 5Al = 6AlB_2 \quad (14)$$

For determining the mechanism of thus reactions, an optical microscopy of the material in an intermediate state has been achieved (figure 1).

Table 3. Gibbs Free Energies of formation for the reaction 1 ÷ 7

T	deltaG1	deltaG2	deltaG3	deltaG4	deltaG5	deltaG6	deltaG7
K	kJ	kJ	kJ	kJ	kJ	kJ	kJ
973.15	-1124	-2474	-1354	-2484	-2127	-1410	-389
998.15	-1131	-2472	-1340	-2514	-2101	-1409	-384
1023.15	-1139	-2470	-1325	-2543	-2075	-1408	-379
1048.15	-1147	-2468	-1311	-2573	-2049	-1408	-374
1073.15	-1156	-2467	-1296	-2602	-2023	-1407	-369
1098.15	-1165	-2466	-1281	-2630	-1997	-1407	-364
1123.15	-1174	-2466	-1267	-2659	-1971	-1407	-359
1148.15	-1187	-2471	-1255	-2687	-1949	-1408	-355
1173.15	-1201	-2479	-1244	-2714	-1930	-1411	-352
1198.15	-1215	-2487	-1232	-2742	-1911	-1413	-348
1223.15	-1230	-2495	-1221	-2769	-1892	-1416	-344
1248.15	-1245	-2504	-1210	-2796	-1873	-1419	-340
1273.15	-1261	-2513	-1199	-2823	-1854	-1422	-336

Table 4. Gibbs Free Energies of formation for the reactions 8 ÷ 14

T	deltaG8	deltaG9	deltaG10	deltaG11	deltaG12	deltaG13	deltaG14
K	kJ	kJ	kJ	kJ	kJ	kJ	kJ
973.15	-2334	-1978	1	-580	-149	-358	-582
998.15	-2364	-1951	0	-579	-150	-355	-579
1023.15	-2393	-1925	-2	-577	-150	-352	-575
1048.15	-2422	-1898	-3	-576	-151	-348	-572
1073.15	-2450	-1872	-5	-574	-151	-345	-569
1098.15	-2478	-1845	-7	-573	-152	-342	-566
1123.15	-2506	-1818	-8	-571	-152	-339	-563
1148.15	-2534	-1797	-10	-570	-153	-336	-560
1173.15	-2561	-1777	-11	-568	-153	-332	-557

T	deltaG8	deltaG9	deltaG10	deltaG11	deltaG12	deltaG13	deltaG14
K	kJ	kJ	kJ	kJ	kJ	kJ	kJ
1198.15	-2588	-1757	-13	-567	-154	-329	-554
1223.15	-2615	-1738	-15	-565	-154	-326	-551
1248.15	-2641	-1718	-16	-564	-155	-322	-547
1273.15	-2667	-1698	-18	-562	-155	-319	-544

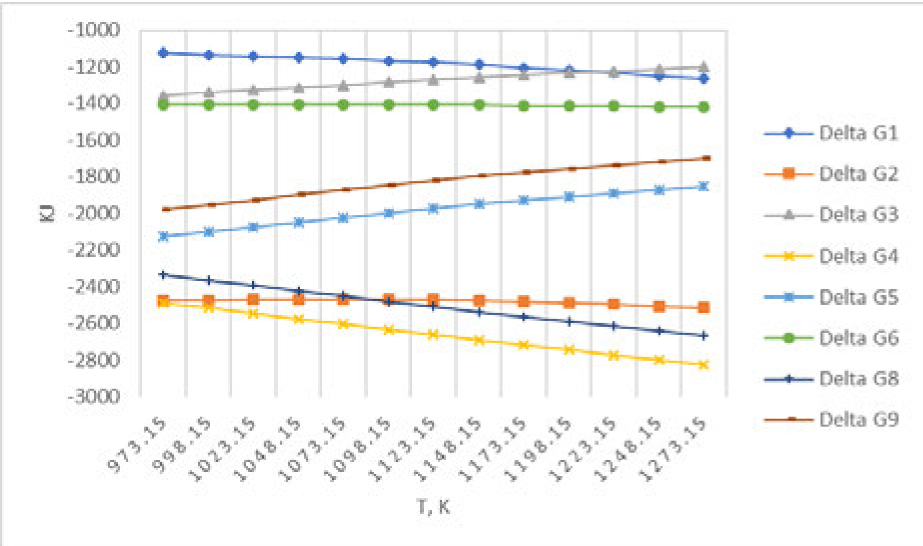

Fig. 2. Variation of standard free enthalpy (ΔG) in the temperature range 973.15 – 1273.15 K of the reactions 1 ÷ 6, 8 and 9.

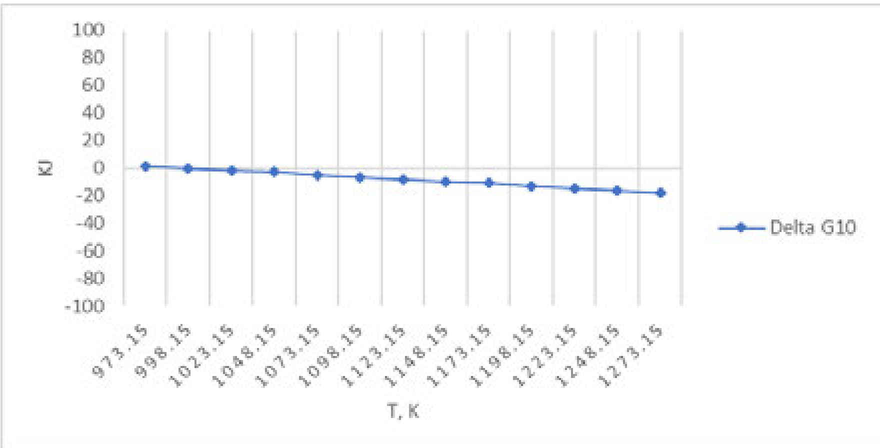

Fig. 3. Variation of standard free enthalpy (ΔG) in the temperature range 973.15 – 1273.15 K of the reaction 10.

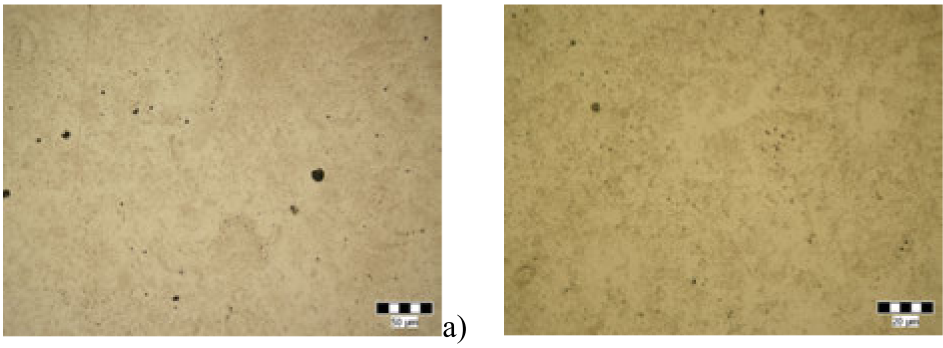

C2 (7050) - reaction time 60 minutes, 5% TiB_2 - a) 200x; b) 500x

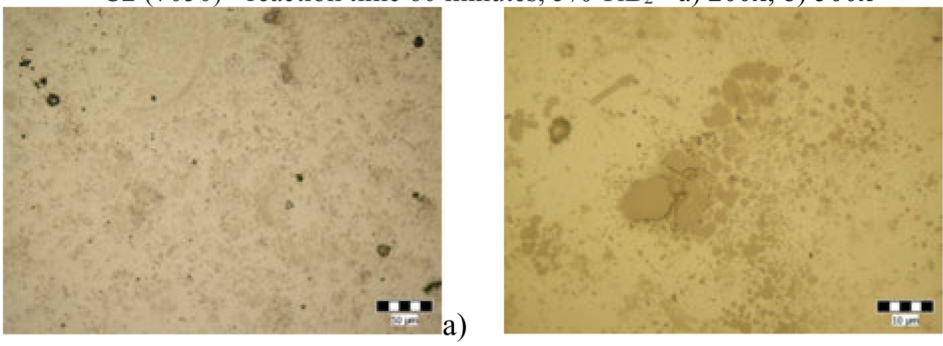

C22 (7050) - reaction time 90 minutes, 5% TiB_2 - a) 200x; (b)1000x

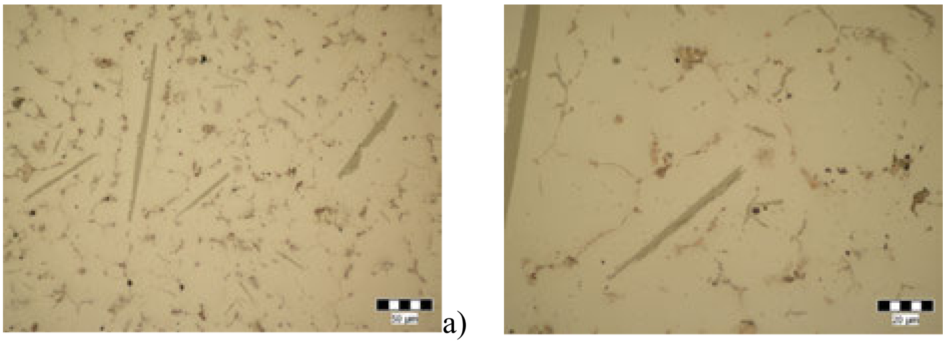

C23 (7050) - reaction time 120 minutes, 5% TiB_2 - a) 200x; (b) 500x

Fig. 4. Optical microstructures of composites with different concentrations of in-situ formed particles.

Increasing the reaction time from 60 to 120 minutes leads to the agglomeration of TiB_2 particles. Also, from the optical microscopy analysis, an increase in the concentration of $TiAl_3$ compounds can be observed at 120 minute reaction times, which means a change in the direction of the reaction (10), with the dissolution of TiB_2.

In order to identify the TiB_2 particles, we performed the diffractometric analysis of the samples. Figures 2, 3 and 4 show the results of the diffractometric analysis for the analyzed samples (5% TiB_2), the list of reaction products present in the analysed samples and the list of the corresponding peakings.

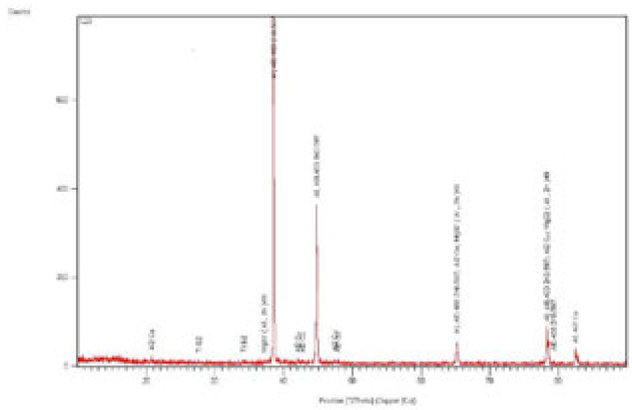

a)

No.	Visible	Ref. Code	Compound N...	Chemical Formula	Score	Scale ...	SemiQua
1	☐	01-071-3760	Aluminum	Al	51	0.465	-
2	☐	00-052-0856	Aluminum Zinc	Al0.403 Zn0.597	23	0.425	-
3	☐	01-089-1980	Khatyrkite, s...	Al2 Cu	Un...	0.021	-
4	☐	01-075-0967	titanium boride	Ti B2	8	0.018	-
5	☐	00-039-0951	Aluminum M...	Mg32 (Al , Zn)49	2	0.039	-

b)

Date: 5/22/2014 Time: 13:36:52 File: C23

No.	Pos. [°2Th.]	d-spacing...	Rel. Int.	FWHM [°...	Matched by	Area [cts*°2Th	Back
1	20.6847	4.29420	0.63	0.1181	01-089-1980	0.89	
2	27.6459	3.22672	0.27	0.1968	01-075-0967	0.38	
3	34.1627	2.62465	0.64	0.2362	01-075-0967	0.91	
4	37.1778	2.41843	0.47	0.1574	00-039-0951	0.66	
5	38.5416	2.33594	100.00	0.1968	01-071-3760; 00-...	141.86	
6	42.0777	2.14745	0.79	0.2362	01-089-1980	1.12	
7	42.7501	2.11522	0.96	0.3149	01-089-1980	1.36	
8	44.8034	2.02294	24.35	0.0984	01-071-3760; 00-...	34.54	
9	47.3701	1.91914	1.08	0.1968	01-089-1980	1.54	
10	47.8646	1.90047	0.59	0.1574	01-089-1980	0.83	
11	65.1685	1.43153	6.63	0.1968	01-071-3760; 00-...	9.40	

c)

XRD crystallites size:
TiB_2 – 19,12 nm
Al – 35,84 nm

Fig. 5. Diffractometric analysis (a) for the sample maintained 60 minutes, the list of compounds (b) and the list of peaks (c) with the crystallite dimensions.

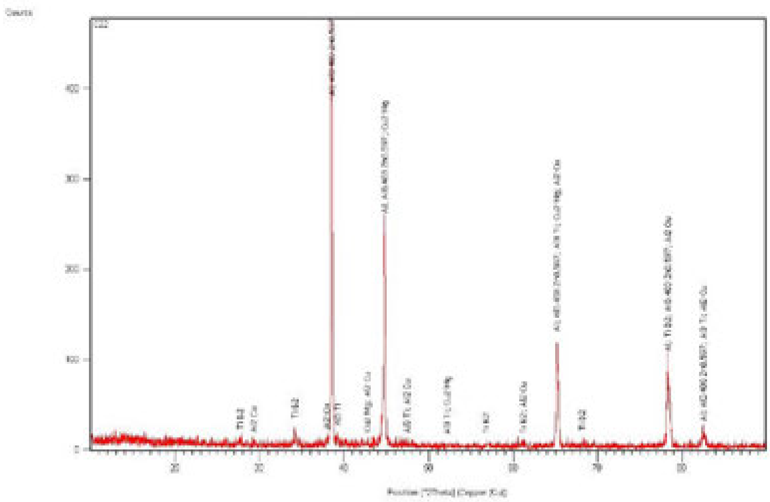

a)

No.	Visible	Ref. Code	Compound N...	Chemical Formula	Score	Scale ...	SemiQua
1	☐	01-089-3657	Aluminum, syn	Al	52	0.684	-
2	☐	01-071-5368	Titanium Bor...	Ti B2	18	0.042	-
3	☐	00-052-0856	Aluminum Zinc	Al0.403 Zn0.597	32	0.457	-
4	☐	03-065-7847	Aluminum Ti...	Al3 Ti	7	0.044	-
5	☐	03-065-9042	Copper Magnes	Cu2 Mg	0	0.079	-
6	☐	01-089-1981	Khatyrkite, s...	Al2 Cu	4	0.011	-

b)

No.	Pos. [°2Th.]	d-spacing ...	Rel. Int.	FWHM [°...	Matched by	Area [cts*°2Th...	Backgr.[cts]	Height [cts]
1	27.6986	3.22070	1.43	0.1574	01-071-5368	0.71	4.81	4.57
2	29.2917	3.04907	1.61	0.3149	01-089-1981	0.80	4.70	2.57
3	34.1764	2.62363	4.01	0.1181	01-071-5368	1.99	4.57	17.09
4	37.9521	2.37085	2.27	0.1968	01-089-1981	1.13	5.21	5.80
5	38.4975	2.33851	100.00	0.1181	01-089-3657; 00-...	49.66	5.23	426.34
6	39.1976	2.29834	2.83	0.1574	03-065-7847	1.41	5.25	9.06
7	42.7516	2.11515	1.14	0.3149	03-065-9042; 01-...	0.57	5.44	1.83
8	44.7704	2.02435	47.98	0.0984	01-089-3657; 00-...	23.83	4.89	245.47
9	47.4100	1.91762	4.46	0.9446	03-065-7847; 01-...	2.22	4.16	2.38
10	52.1691	1.75334	0.39	0.1181	03-065-7847; 03-...	0.19	3.38	1.65
11	56.7708	1.62166	2.58	0.6298	01-071-5368	1.28	2.95	2.06
12	61.2021	1.51444	2.71	0.4723	01-071-5368; 01-...	1.35	3.08	2.89
13	65.1708	1.43149	31.62	0.1378	01-089-3657; 00-...	15.70	3.74	115.55
14	68.1258	1.37642	0.82	0.0984	01-071-5368	0.41	3.82	4.22
15	78.2786	1.22036	47.99	0.1920	01-089-3657; 01-...	23.83	3.74	93.10
16	82.5082	1.16818	5.96	0.1440	01-089-3657; 00-...	2.96	3.75	15.41

XRD crystallites size:
TiB_2 – 31,68nm
Al – 35,79nm
$TiAl_3$ – 31,49nm

c)

Fig. 6. Diffractometric analysis (a) for the sample maintained 90 minutes, the list of compounds (b) and the list of peaks (c) with the crystallite dimensions.

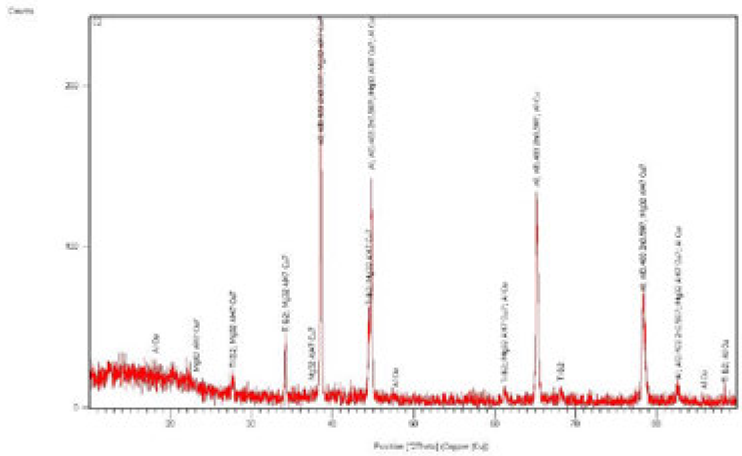

a)

No.	Visible	Ref. Code	Compound N...	Chemical Formula	Score	Scale ...	SemiQua
1	☐	01-071-4624	Aluminum	Al	49	1.067	-
2	☐	01-075-1045	titanium boride	Ti B2	39	0.200	-
3	☐	00-052-0856	Aluminum Zinc	Al0.403 Zn0.597	29	0.627	-
4	☐	00-019-0011	Aluminum C...	Mg32 Al47 Cu7	7	0.701	-
5	☐	01-088-1713	Cupalite, syn	Al Cu	6	0.376	-

b)

Date: 5/22/2014 Time: 13:28:22 File: C2

No.	Pos. [°2Th.]	d-spacing...	Rel. Int.	FWHM [°...	Matched by	Area [cts*°2Th	Backg
1	18.0833	4.90565	2.78	0.1181	01-088-1713	1.14	
2	23.1844	3.83657	1.74	0.1378	00-019-0011	0.71	
3	27.7015	3.22038	6.36	0.2362	01-075-1045; 00-...	2.60	
4	34.1691	2.62417	10.11	0.1181	01-075-1045; 00-...	4.13	
5	37.4436	2.40187	1.82	0.1574	00-019-0011	0.74	
6	38.5175	2.33734	69.05	0.1181	01-071-4624; 00-...	28.19	
7	44.4752	2.03710	14.98	0.1181	01-075-1045; 00-...	6.12	
8	44.7865	2.02366	32.59	0.0984	01-071-4624; 00-...	13.31	
9	47.7200	1.90589	2.81	0.6298	01-088-1713	1.15	
10	61.1936	1.51463	4.08	0.3149	01-075-1045; 00-...	1.67	
11	65.1740	1.43024	100.00	0.2400	01-071-4624; 00-...	40.83	
12	68.1182	1.37542	5.53	0.2880	01-075-1045	2.26	
13	78.2696	1.22048	38.76	0.1920	01-071-4624; 00-...	15.82	

c)

XRD crystallites size:
TiB_2 – 29,65 nm
Al – 31,17 nm

Fig. 7. Diffractometric analysis (a) for the sample maintained 120 minutes, the list of compounds (b) and the list of peaks (c) with the crystallite dimensions.

4. Characterization of TiB_2 particles

After leaching in HCl of the composite and successive washings of solid material obtained, particles were analysed through X-ray diffraction (X-ray diffractometer – X'Pert PRO MPD, PANalytical) and fluorescence (X-ray Fluorescence Spectrometer – S8 Tiger). Form and dimensions of the TiB_2 particles were determined by Transmission Electron Microscopy (TEM) and through DLS technique (Dynamic Light Scattering – Zetasizer Nano ZS Malvern). The samples were spread in distilled water, homogenized in an ultrasonic box at different times. The amount of sample taken for the measurement was 1 ml and the temperature 25°C. Particle sizes were determined according to the intensity of the scattered light and the volume.

No.	Visible	Ref. Code	Compound N…	Chemical Formula	Score
1	☑	04-004-5881	Titanium Bo…	Ti B2	75
2	☑	04-006-2601	Copper, syn	Cu	55
3	☑	04-012-6327	Copper Oxide	Cu2 O	48
4	☑	01-088-2487	Quartz, syn	Si O2	24

a)

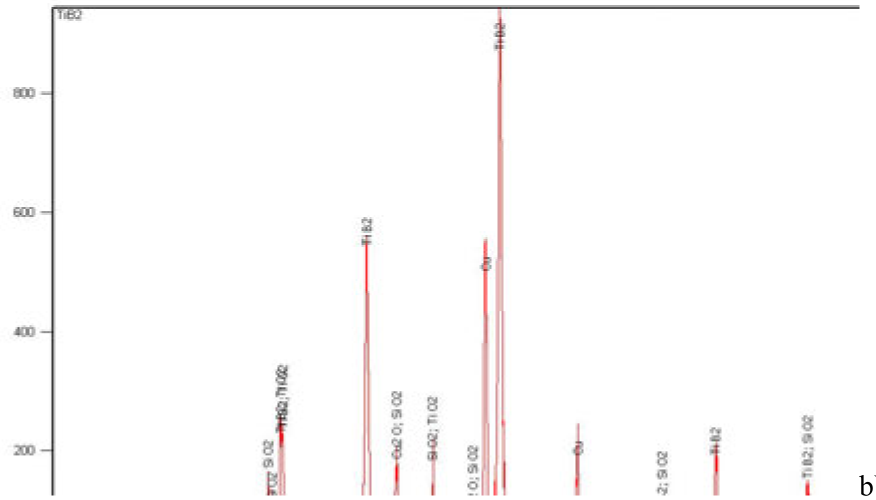

b)

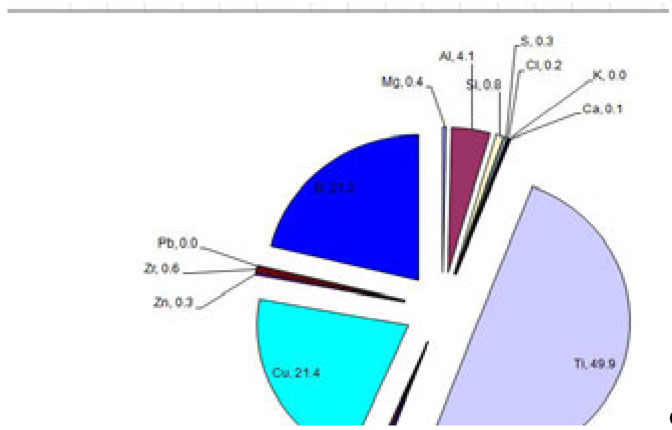

c)

Fig. 8. Analysis of TiB_2 powders obtained:
a), b) - compound distribution (quantitative) and XRD diagram; c) elemental distribution.

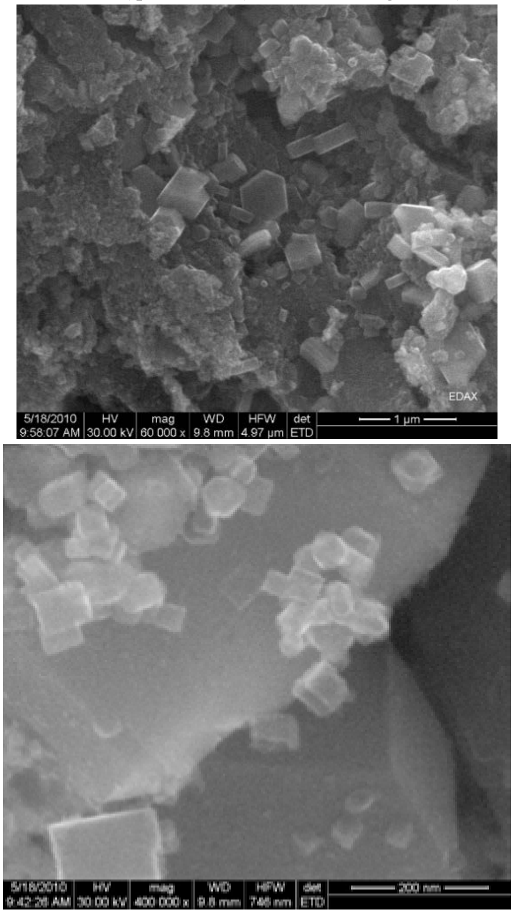

Fig. 9. The morphology of the TiB_2 particles,
examined using transmission electron microscopy (TEM).

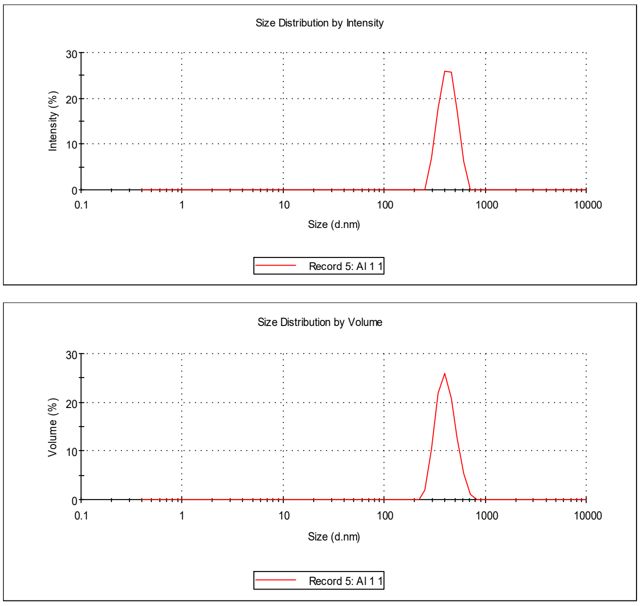

Size	Intensity
d.nm	%
295.3	6.9
342	17.8
396.1	25.9
458.7	25.7
531.2	17.4
615.1	6.3

Fig. 10. Dimensional analysis of TiB_2 powders, determined by the DLS technique (dispersed particles) - Zetasizer Nano ZS Malvern.

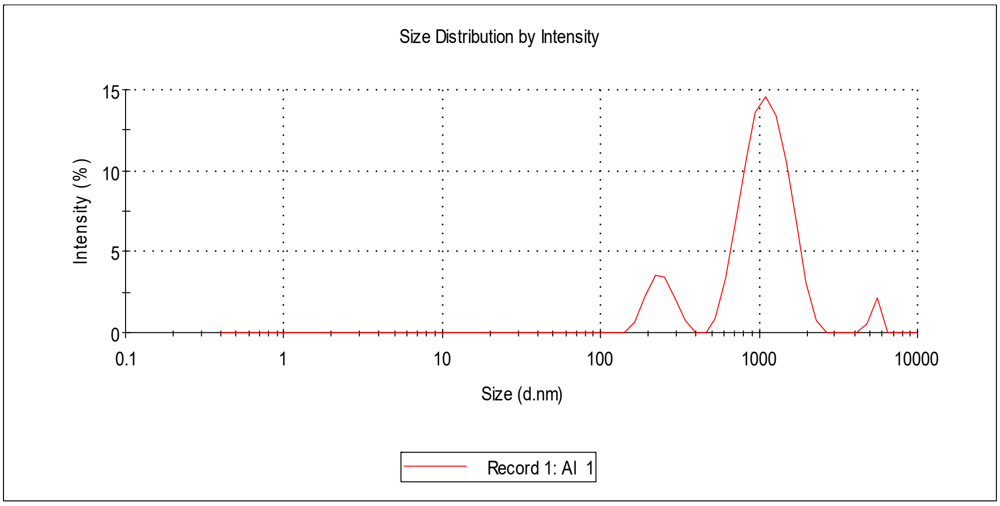

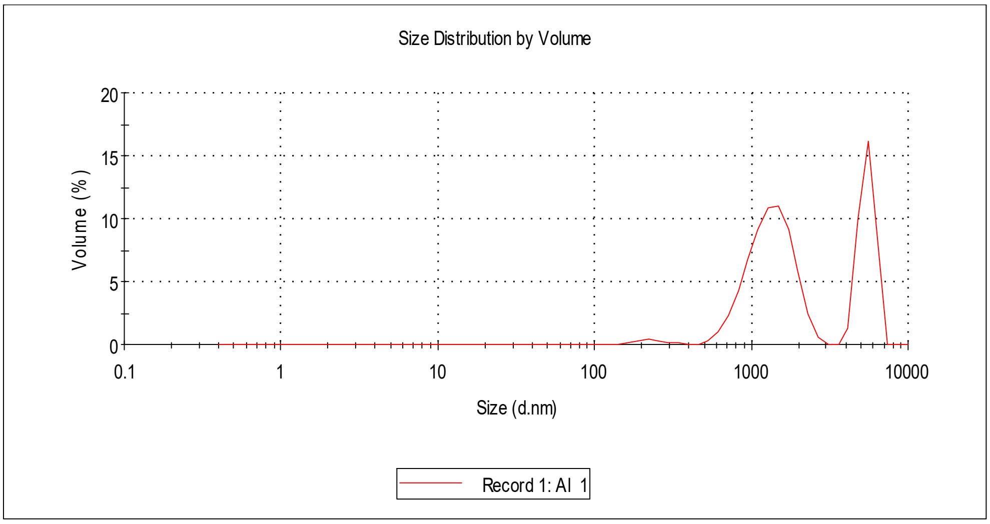

Size	Intensity	Size	Intensity	Size	Intensity
d.nm	%	d.nm	%	d.nm	%
164,2	0.7	531.2	0.9	1281	13.4
190.1	2.3	615.1	3.3	1484	10.5
220.2	3.5	712.4	7	1718	6.7
255	3.4	825	10.8	1990	3.1
295.3	2.2	955.4	13.6	2305	0.8
342	0.8	1106	14.6	4801	0.5
				5560	2.1

Fig. 11. Dimensional analysis of TiB_2 powders, determined by the DLS technique (agglomerated particles) - Zetasizer Nano ZS Malvern.

5. Conclusions

1) In-situ AA 7050 / TiB_2 by reaction between potassium hexafluorotitanate (K_2TiF_6) and potassium tetrafluoroborate (KBF_4) are fabricated at 750^{o}C.
2) Thermodynamic data, computed with HSC Chemistry program, indicates the possibility of TiB_2, Al_3Ti, AlB_2, AlB_{12}, MgB_2 and MgB_{12} compounds formation, with negative ΔG^o_T.

3) To highlight the mechanism of TiB_2 particle formation three time of reaction (60, 90 and 120 min.) were studied. Increasing the reaction time from 60 to 120 minutes leads to agglomeration of TiB_2 particles. Also, an incease of Al_3Ti concentration at 120 minute on observe by optical micrographies as a result of shifting the reaction (10) from right to left.
4) The XRD patterns revealed the formation of TiB_2. Form and dimensions of TiB_2 particles obtained after separation from aluminium matrix were determined by Transmission Electron Microscopy (TEM) and through Dynamic Light Scattering (Zetasizer Nano ZS Malvern).
5) Only aluminium and magnesium from AlCuMgZn alloy can interacts with salts (K_2TiF_6 and KBF_4), but the influence of magnesium is negligible.

References

[1] Moldovan P., *Compozite cu matrice metalică*, Editura PRINTECH, Bucureşti, 2008, p. 17.
[2] Zhao D.G., Liu X.F., Pan Y.C., Bian X.F., Liu X.J., *Microstructure and mechanical properties of in situ synthesized (TiB_2+Al_2O_3)/Al-Cu composites*, J. Mater. Process. Technol., **189**, Issue 1-3, 6 July 2007, p. 237-241.
[3] Geng J., Liu G., Hong T., Wang M., Chen D., Ma N., Wang H., *Tuning the microstructure features of* in-situ *nano TiB_2/Al-Cu-Mg composites to enhance mechanical properties*, Journal of Alloys and Compounds, **775**, 15 February 2019, p. 193-201.
[4] Ma Y., Geng J., Chen Z., Wang M., Chen D., Ji G., Ji V., Wang H., *Experimental study of the mechanisms of nanoparticle influencing the fatigue crack growth in an* in-situ *TiB_2/Al-Zn-Mg-Cu composite*, Engineering Fracture Mechanics, **207**, 15 February 2019, p. 23-35.
[5] Mohanavel V., Rajan K., Arul C., Senthil P.V., *Production, Microstructure and Mechanical behavior of AA6351/TiB_2 composite synthesized by direct melt reaction method*, Materials Today, Proceedings, Vol. 4, 2017, p. 3315–3324.
[6] Ramesh C.S., Pramod S., Keshavamurthy R., *A study on microstructure and mechanical properties of Al 6063 - TiB_2 in situ composites*, Mater. Sci. Eng. A, **528**, Issue 12, February 2011, p. 4125-4132.
[7] Kumar S., Chakraborty M., Sarma V.S., Murty B.S., *Tensile and wear behaviour of in situ Al-7Si/TiB_2 particulate composites*, Wear, **265**, 2008, p. 134-142.
[8] Moldovan P., Butu M., Popescu G., Buzatu M., Usurelu E., Soare V., Mitrica D., *Thermodynamics of interactions in Al-K_2TiF_6-KBF_4 system*, Rev. Chim. (Bucharest), **61**, Vol. 9, 2010, p. 828-832.
[9] Ramesh C.S., Ahamed A., Channabasappa B.H., Keshavamurthy R., *Development of Al 6063 - TiB_2 in situ composites*, Materials and Design, **31**, 2010, p. 2230-2236.
[10] Fan T., Yang G., Zhang D., *Thermodynamic effect of alloying addition on in situ reinforced TiB_2/Al composites*, Metallurgical and Materials Transactions A, **36**, Issue 1, February 2005, p. 225-233.
[11] Rajan M., Ramabalan S., Dinaharan I., Vijay S.J., *Synthesis and characterisation of in situ formed titanium diboride particulate reinforced AA 7075 aluminum alloy cast composites*, Materials and Design, Vol. 44, 2013, p. 438-445.
[12] Butu M., Moldovan P., Marcu F.D., Berbecaru A., Stancel C.D., Rosu L., Ungureanu I., *Thermodynamics of in situ production of aluminium matrix composites. Comparative analysis*, Rev. Materiale Plastice Vol. 53, Issue 3, 2016, p. 428-433.
[13] Buțu M., Moldovan P., Ușurelu E., Mitrică D., *The mechanism and kinetics of TiB_2 nanoparticles and microparticles formation via aluminothermic reaction*, Rev. Chim. (Bucharest), 62, Vol. 7, 2011, p. 723-726.
[14] Vivekanada A. S., Balasivanandha Prabu S., Paskaramoorthy R., *Influence of process parameters of aluminothermic reduction process on grain refinement of in-situ Al/TiB_2 composites*, Materials Today, Proceedings, Vol. 5, Issue 1, 2018, p. 1071-1075.

[15] Han Y., Liu X., Bian X., *In situ TiB_2 particulate reinforced near eutectic Al-Si alloy composites*, Composites, Part A, Vol. 33, March 2002, p. 439-444.
[16] Zolotorevsky V. S., Belov N. A., Glazoff M. V., *Casting aluminium alloys*, Elsevier Science, 2007, p. 544.